Evaluation of Resistivity Index Methods - A North Sea Case Study

Anthony J Purpich
Mobil North Sea Limited, Aberdeen, Scotland
John A Nieto*
Mobil North Sea Limited, London, England
Robert J Evans
Simon-Robertson, Aberdeen, Scotland

ABSTRACT

Resistivity index (I) was measured on a suite of sandstone plugs cut from preserved cores from North Sea Jurassic and Triassic reservoirs. Duplicate plugs were drilled at each horizon and prepared by soxhlet extraction and oven drying. A set was saturated with brine, desaturated and flooded with crude oil. Ageing for 1000 hours at reservoir temperature followed. Cleaned and aged plugs were available for resistivity index testing.

Resistivity index was determined on cleaned plug sets using an air-brine porous-plate technique, and on the aged plugs using a crude oil-brine continuous injection method. The porous-plate, drainage, I data were determined at both ambient and effective reservoir stress using a four-electrode cell. Air displaced brine during the tests. The continuous injection I data were measured at effective reservoir stress using a two-electrode cell. The samples were initially at irreducible water saturation (S_{wi}), containing brine and crude oil. Brine displaced crude oil in the tests.

Several I-S_w curve shapes were observed in the porous-plate and continuous injection tests. Both linear and "discontinuous" trends were observed in the porous-plate ambient data, whereas linear trends dominated the porous-plate effective reservoir stress data. The discontinuity in the porous-plate data occurs when the continuous brine film ruptures during desaturation, allowing air, the non-wetting phase, to contact the grains. The plugs used for continuous injection were rendered moderately to strongly oil-wet by the ageing process. "Knee" and "sigmoidal" trends dominated the continuous injection data with both "knee" and "sigmoidal" inflexion points occurring at about 34% S_w. The "knee" and "sigmoid inflexion point" are believed to occur at the point where the injected brine becomes a continuous phase, thus dramatically improving the electrical path. Curve type did not correlate with pore geometry.

The saturation exponent from the porous-plate tests increased with effective reservoir stress when a least-squares fit of the data was used. However, no change was observed when using a two-point method, which uses I at S_{wi}. The value of n determined from the 2-point method does not change appreciably due to measurement method (porous-plate or continuous injection).

The 2-point method of deriving n is recommended for use in estimating initial water saturation in reservoirs of the type studied. This is a pragmatic approach which allows evaluation in non-Archie situations. However, the fluids used in the testing, their distribution, and the S_{wi} reached, must be similar to those found in the reservoir.

**Currently with Mobil Research and Development Corporation, Dallas, Texas*

INTRODUCTION

An extensive study was made with the aim of gaining a better insight into laboratory resistivity index measurements. The purpose of this study was to examine the electrical properties of the reservoir sands with the goal of enhancing reservoir description and management. Knowledge of the variance in petrophysical parameters caused by measurement technique, stress and wettability conditions was important, since the reservoirs are known to be neutral to moderately oil-wet. Since the study was to be used for field application it was important that the measurements be made on cores from the producing horizons, and that the reservoir conditions be duplicated, within practical limits. Over 60 plugs were used in the study. Electrical measurements were made on clean and aged samples using both two- and four-electrode systems. Ambient and effective reservoir stress conditions have been employed, after Nieto et al. (1990). Core samples were recovered from several wells in a producing oil field in the Central Graben area of the UK sector of the North Sea. The core samples are from consolidated sandstone formations of Jurassic and Triassic age, which, with one exception, were drilled with oil-base mud. These formations are divided in seven reservoir units.

The Jurassic sandstones are classified as sublithic arenites whereas the Triassic sandstones are subarkosic to arkosic arenites. Grain size ranges from fine to very coarse. Detrital minerals are quartz, with minor to significant amounts of feldspars, lithic fragments, and micas in minor amounts. The feldspars have undergone partial to complete dissolution. In order of abundance, the feldspars present are orthoclase, plagioclase, microcline and perthite. The sandstones are cemented with ferroan dolomite and calcite, siderite, kaolinite, and silica. Jurassic reservoir quality is very good (Table 1) with an average porosity of 17% and permeability of 560 mD. Triassic reservoir quality is variable with an average porosity of 17% and permeability of 228 mD. The cation-exchange capacity of both Jurassic and Triassic sandstones is low, with an average of 0.131 meq/CC and a Triassic average of 0.104 meq/CC..

REVIEW OF PAST WORK

Archie's equation is the basis of log-derived water saturation. The resistivity index (I) is defined as the ratio of the resistivity of the partially brine-saturated rock to the 100% brine-saturated rock. The saturation exponent (n) is defined as the slope in the double-logarithmic plot of I versus water saturation (S_W). One form of the Archie equation is:

$$S_W^{-n} = I = [R_t/R_O]$$

In this empirical relationship, several critical assumptions are implicit. Firstly, the grains or matrix must not be conductive. Secondly, the pore size distribution must be unimodal, and thirdly, "the relationship between the poor sizes and the pore aperture sizes [must vary] in a regular way" (Herrick, 1988). The conductive brine film must also be continuous.

Many workers have investigated the effects of wettability, clay, pore size distribution, and measurement method on connate water saturation and the resistivity index. To study the affects of wettability and saturation history, many experimentalists have induced hydrophobic and hydrophilic behaviour using special chemical treatments. Glass beads, Teflon, Berea sandstone and reservoir core samples have been used with air, brine, mercury, various oils and methanol with varying success. Additionally, mathematical models have been used to try to explain the anomalies associated with electrical behaviour in rocks.

As early as 1953, Keller concluded that the Archie equation is "inadequate to describe the resistivity of rocks at low water saturation". He surmised that the increase in the laboratory resistivity (R_t) with decreasing water saturation, is a result of the diminishing cross-sectional area of the water film. Mungan and Moore (1968) and Anderson (1986) remind us that the Archie equation is an empirical relationship based on data from strongly water-wet rocks. The length of conductive path as well as the cross-sectional area affects resistivity. Anderson (1986) also states that the Archie equation is "non-unique" once the reservoir wettability is altered.

In 1982, Melrose wrote that reservoir wettability can be predicted by comparing the connate water saturation and the saturation required to fill all the pores smaller than the critical size for stable films. As a water-filled system is desaturated, the brine will be displaced first in the larger pores, then in successively smaller and smaller pores. Below some critical saturation, the otherwise stable wetting film breaks. This occurs non-uniformly, affecting only portions of the grain surfaces.

Craig (1971) offered several "rules of thumb" on wettability. Generally, water-wet rocks have initial water saturations greater than 20 to 25%, whereas oil-wet rocks have S_W's less than 15% and often below 10%.

Often, the I-S_W data in the double-logarithmic crossplots do not form a linear trend. Based on porous-plate experiments and mercury injection data, Swanson (1985) explained that curvature in resistivity index data could be caused by micropores as well as conductive clays. Worthington et al.(1988) found that the saturation index measured in preserved samples, increased after drying and resaturation. They attributed this to the collapse of the authigenic clays, thus changing the pore size distribution. Using a numerical approach, Lyle and Mills (1989) showed that a non-uniform saturation alone will cause curvature in the I-S_W trend. Sprunt (1991) showed that non-linearities could be due to errors in porosity measurements.

Both two- and four-electrode configurations are commonly used to measure electrical resistivity in the laboratory. A 2-electrode cell was considered advantageous by Worthington et al. (1990) due to simplicity of design and the ability to measure the resistivity across the entire sample. Worthington et al. noted that while the 4-electrode method does not have severe electrical coupling problems, a uniform saturation distribution is required. Mahmood et al. (1991) found that the 2-electrode cell sometimes yields higher values of n than the 4-electrode technique. Further, they concluded that the saturation history has the greatest impact on n, followed by temperature and to a lesser degree, pressure. de Waal et al. (1991) and Sprunt et al. (1991), using X-ray CT scanning, showed that n varied with the saturation distribution. Two- and four-electrode systems, respectively, were used by the researchers.

The relationship between n and wettability has also been investigated. Donaldson et al. (1989) observed a linear relationship between the saturation exponent and the USBM wettability index. He also noted that "oil/water/rock systems become more water-wet as the temperature is increased." Sharma et al. (1991) note that wettability has a significant effect on the resistivity index measurement, particularly in rocks with poorly connected pores, and non-uniform pore size distributions. Additionally, the effects of saturation hysteresis are more pronounced in oil-wet rocks. Sharma's experiments were carried out on Berea core and glass beads, treated to enhance hydrophobic and hydrophilic behaviour.

The direction of saturation change as well as the fluids used, affect the laboratory derived n (Longeron et al., 1989, Sharma et al. 1991, Wei et al., 1991). The hysteresis phenomenon is caused by a change in the saturation distribution between drainage and imbibition runs. Longeron et al. (1989) recommended that the drainage-derived n be used for calculating S_W at original conditions, and that the imbibition curve be used for S_W in waterflood conditions. They also noted that a gas-brine system gave a lower n than an oil-brine system.

Worthington, Pallat and Toussaint-Jackson (1989) showed that n measured over a limited S_W range may not be representative of a different range.

LABORATORY METHODS

The following section provides an overview of the test methods used. A more detailed description is provided in the Appendix.

Cleaning and Basic Measurements

The majority of the samples in the study came from preserved whole core samples. Duplicate 1 1/2-inch plugs were cut at each depth, using brine to cool and lubricate the bit, and visually examined to ensure consistency among the samples. The plugs were thoroughly cleaned and dried in a vacuum oven at 60°C until constant weight was attained.

Ambient, helium-expansion porosity and gas permeability were determined for each sample prior to the resistivity testing. The samples were again checked for consistency, and those exhibiting heterogeneity were removed from the set.

Wettability

Cleaned plugs: Wettability was determined using the Combined Amott/USBM Method. The samples were first desaturated to irreducible water saturation (S_{Wi}) using a porous-plate, then flooded with kerosene. The permeability to oil at S_{Wi} was then measured. The plugs were placed under simulated formation brine and allowed to imbibe spontaneously, followed by centrifugation in which brine displaced oil. Centrifuge speed was increased incrementally, and data to determine capillary pressure were recorded.

Lastly, the samples were flushed with brine, driving the plugs to residual oil saturation (S_{ro}). The spontaneous imbibition and centrifuge processes were repeated using oil to displace the brine.

Aged plugs: A second set of plugs was aged, and wettability determined using the Combined Amott/USBM Method. The procedure followed for the cleaned plugs was also used here, with the exception that the crude oil from the ageing process was displaced with depolarised kerosene.

Cation Exchange Capacity

The ends trimmed from the plug samples for electrical measurements were used for cation exchange capacity (CEC) determination. The trimmed ends were disaggregated, cleaned of oil, and dispersed in sodium acetate. The dispersed particles were then saturated with sodium cations by shaking the samples for 20 minutes in the solution followed by centrifugation. The process was repeated four times followed by removal of excess reagent from the samples. The sodium ions were replaced with ammonium cations and the volume of the former was measured by flame photometry.

Cleaned-State, Resistivity Index Measurements

Cleaned and dried plugs were initially saturated with filtered, simulated formation brine. Two brines were used to accommodate the different field waters. Formation resistivity factor at ambient conditions was measured using a four-electrode cell (Figure 2). Several readings were taken for each sample over a three day period, until consecutive readings varied less than 2%.

Porous-plate, ambient conditions: Air-brine capillary pressure, in conjunction with resistivity index, was performed next using a porous-plate technique. Core resistance was measured at each pressure using a 4-electrode cell (Figure 2), once an equilibrium saturation had been reached. A maximum air-brine capillary pressure of 200 psi was applied. Sample saturation was determined gravimetrically at each step. The samples were resaturated upon completion of the test and again weighed.

Porous-plate, effective reservoir stress: Each saturated plug was mounted in a cell and the confining pressure increased incrementally to 5100 psi, which represents the effective reservoir stress (Figure 3). The pore volume change and formation resistivity factor were determined at salient points. As in the ambient tests, the plugs were desaturated using air-brine and a porous-plate. Resistance was measured at each step, using a 4-electrode cell, and resistivity index calculated. The capillary pressure curve was determined in conjunction with the I measurements. The final water saturation was measured using Dean-Stark extraction as a check on capillary pressure data.

Aged-State, Resistivity Index Measurements

One set of twinned plugs was cleaned, dried, and saturated with brine, then desaturated using a porous-plate. The voided pore space was filled with dead crude oil, and the plugs were aged in a chamber for 1000 hours at reservoir temperature, 200°F.

Continuous injection, effective reservoir stress: After ageing, the samples were loaded into individual core holders and a confining stress of 5100 psi applied. Brine was then injected into the core at a flow rate equivalent to one pore volume through-put over a 14 day period. Resistance was measured as the brine saturation increased. Figure 4 is a schematic of the laboratory equipment.

R_O was not measured since the aged plugs contained brine and oil at all times. In order to define R_O, the plug resistivity (R_t) was plotted against water saturation (S_W) as brine displaced oil, and extrapolated to 100% S_W. The resulting R_O value was recorded and the resistivity index calculated using:

$$I = (R_t/R_O)$$

Upon completion of the continuous injection experiments, the samples were cleaned, saturated with brine, and desaturated using a porous-plate. Resistivity at irreducible water saturation was determined with the samples at 5100 psi confining stress.

RESULTS

A variety of I-S_W curves are seen in the porous-plate and continuous injection data. The curve shapes observed in the continuous injection tests are unique to this method, with the exception of the typical Archie linear I-S_W trend. Recall that in the porous-plate experiments, air displaced brine, while in the continuous injection work, brine displaced crude oil.

Cleaned-State, Porous Plate Measurements

Thirty one samples were tested using the porous-plate technique. One third of the ambient I-S_W data exhibit a straight-line trend, which is present over the range of water saturations investigated (Figure 5). An average Archie saturation exponent (n) of 1.75 was derived from these data using a least-squares fit.

Two additional trends were observed, which we have termed "Discontinuous" and "Anomalous". The "Discontinuous" trend exhibits a resistivity index that increases sharply at low water saturations (Figure 6). In the "Anomalous", the data are generally linear, but "noisy". These trends were observed equally in the remaining two-thirds of the samples. The discontinuity in the "Discontinuous" trend was observed over a range of water saturation values between 12 and 28%, Figure 6 illustrates an S_W value of 25%.

Rock parameters have been examined to help identify consistent relationships. To date, no clear relationship has been found in this data set, between rock parameters and curve shapes. Some of the rock parameters used were "Pore Geometry Factor", grain density, porosity, permeability, water saturation and wettability. The values of some of these parameters for each "trend" are summarised in Tables 2 and 3.

"Pore Geometry Factor" (after Leverett, 1941) is calculated using the relationship:

$$PGF = \sqrt{K/\phi} \ .$$

Clearly, PGF alone does not determine the shape of the I-S_W trend, although it can be seen that the "Linear" plugs tend to be of lower reservoir quality, whereas the "Anomalous" can be from any reservoir (Figure 7). The "Discontinuous" and "Linear" plugs have grain-density modal values of 2.65 g/cm^3 whereas the "Anomalous" samples show a wide distribution (Figure 8).

"Discontinuous" plugs show a bimodal grain-density distribution, with peaks at 2.63 and 2.65 g/cm^3, whereas the PGF was normally distributed.

Irreducible water saturation and Amott wettability-to-water (A_{WW}) do not vary significantly by trend.

Since in this study, we were interested primarily in the reservoir saturation exponent at S_{wi} conditions, a two-point n was derived (after Soendenaa et al., 1989). For each plug, an n was determined by a line between 100% S_w and S_{wi} conditions. These measurements gave saturation exponents that on average are 6% higher than the least-squares fit. A typical result is shown in Figure 9.

Effective reservoir stress was then applied to the plugs. Overall, the saturation exponent increased when using a least-squares fit through the data. However, when the 2-point n was used, no preferential change with effective reservoir stress was observed. Figure 10 compares the changes in saturation exponent with effective reservoir stress for the least-squares fit and 2-point methods; all data are used regardless of trend type.

Changes in curve shape with effective reservoir stress occurred predominantly in the "Discontinuous" samples. The data generally became linear under effective reservoir stress conditions, with an average saturation exponent value of 1.78, which is similar to the straight-line data as shown previously in Figure 5, and in Figure 11. However, n determined from the "Anomalous" data using both least-squares and 2-point methods, increased with effective reservoir stress (Figure 12).

The "Linear" data have a normal PGF distribution whereas the "Anomalous" data remain scattered (Figure 13). The "Discontinuous" plugs that remained unchanged with effective reservoir stress, are lower quality rocks with low PGF's. Figure 14 illustrates the plug grain-densities associated with the porous-plate trends at effective reservoir stress.

Aged-State, Continuous Injection Measurements

As with the porous-plate measurements, distinct curve types resulted from the aged-state continuous injection measurements.

Four dominant trends were observed in the I-S_w plot data.

- A convex-up, discontinuous trend which we have termed "Knee", as shown in Figure 15.
- A "sigmoidal", discontinuous trend which we have termed "S", shown in Figure 16.
- A predominantly "linear" trend as observed in the porous-plate measurements. Figure 17 shows a typical result.
- "Anomalous", which does not follow any distinct trend. A typical example is shown in Figure 18.

As with the porous-plate measurements, no correlation between curve type and rock parameters was seen in the data set. The ageing process however, increased the Amott wettability-to-oil (A_{WO}), and decreased the wettability-to-water (A_{WW}). Figure 19 shows that A_{WO}, initially zero in many of the samples, increased markedly with ageing. Furthermore, an increase in plug resistivity (R_t) at S_{wi}, was observed with increasing oil wettability (Figure 20). General patterns based on "trend" were observed (Figure 20).

Examination of Pore Geometry Factor and plug grain-density, sorted by "trend", shows that curve type is not associated with either (Figures 21 and 22). The "Linear" plugs tend to be poorer quality rocks, due to dolomite cement, exhibiting low PGF's and high grain densities of 2.67 and 2.68 g/cm^3. The PGF distribution of the "Knee" trend is predominantly bimodal, whereas the grain-density distribution is normal. The "S" and "Anomalous" plugs have broad PGF distributions, but the "S" samples tend to have values similar to the "Knee" trends. The "S" plugs are restricted to grain densities of 2.64 and 2.65 g/cm^3, whereas the "Anomalous" plugs range from 2.62 to 2.66 g/cm^3, with no modal value. Table 4 shows averages of some of the rock parameters for the "trends".

Saturation exponents are not clearly defined except for the '"Linear" trend where the average is 1.70. For the other trends n varies with the water saturation. A range of n between 1.06 and 3.39 could be picked from either the "Knee", "S" or "Anomalous" trends.

Comparisons were made between the porous-plate and the continuous injection n's to see if there were systematic changes. Figure 23 is a comparison of the 2-point n's from the effective reservoir stress, porous-plate and continuous injection tests. A dependency on measurement method is not observed in the plot. A second comparison was made using four sets of duplicate plugs, chosen so that the difference in PGF's between duplicates was less than 1%. Figure 24 illustrates that the 2-point n is not dependent on the measurement method.

Figure 25 is an I-S_W plot using two plugs from the same depth with equivalent PGF's, thus homogeneity can be assumed. The purpose of this plot is to illustrate that the I-S_W "trends" may vary with measurement technique and state of wettability. Recall that cleaned-state samples were used in the porous-plate testing, and that aged samples were used in the continuous injection tests. It is clear from the figure that while the S_{wi}'s are similar, the I's are not. A likely explanation is that the brine distribution in the aged plug is different from that in the cleaned plug, resulting in a different plug resistivity at S_{wi} being measured.

In order to use this data for petrophysical evaluation, some explanation and reconciliation of the data must be made.

DISCUSSION

Two resistivity index techniques have been employed. Cleaned samples were measured using porous-plate desaturation (capillary pressure equilibrium), at ambient and effective reservoir stress conditions. Aged samples were measured using a continuous injection method at effective reservoir stress. A 4-electrode cell was used for the porous-plate measurements whereas a 2-electrode cell was used for the continuous injection measurements.

It should be noted that oil displaced water in the porous-plate measurements. Water displaced oil in the continuous injection tests.

Multiple curve shapes seen in the double-logarithmic I-S_W plots, point to the complex nature of the measurements and rock-fluid systems.

Cleaned-State

Porous-plate data: Samples exhibiting linear I-S_w trends need no explanation, except to say that the plugs are typical Archie rocks.

The "Discontinuous" plugs, however, exhibit non-Archie electrical behaviour (Herrick, 1988). The sudden upward curvature in resistivity index at low brine saturations may be explained in the following way. Melrose (1982) pointed out that as a water-filled system is desaturated, the brine will be displaced first from the larger pores, then successively from smaller and smaller pores. With continuing desaturation, it is possible that the brine film may rupture causing the air to contact the grains. The rupture however may not be uniform, leaving some grain surfaces brine wet, and others wetted by air. This complex interaction is dependent on the wettability preference of the rock, which is partially controlled by mineralogy, and is described by Anderson (1986) as "fractional wettability". For clarity, the term "mixed wettability" is used in rocks with water-wet micropores and oil or air-wet macropores.

The rupture in the brine layer creates an electrical discontinuity, which causes the resistivity to increase more rapidly than it might otherwise. Figure 26 illustrates a pore system in which a continuous brine film has ruptured resulting in the non-wetting phase coming into contact with the grains. This is clearly a non-Archie situation, and results in isolated volumes of water that are not in electrical contact with the remaining conducting phases.

Non-linear I-S_w trends are the result of non-Archie conditions. The reason for this is the incompatibility of the plotted parameters. For example, in a rock desaturated to the point where the stable brine film ruptures, the brine that remains contiguous, and therefore conductive, can be termed "electrically-effective". That is, it is conducting electrical current. Non-conducting, isolated brine, whether confined to micropores or residing on grains, can be termed "ineffective". The isolated brine though, remains part of the measured total brine volume of the plug. Thus, a plot of total brine saturation versus resistivity index will be non-linear. An improved plot would consist of I versus the "electrically effective" water saturation. We assert that if the "electrically effective" brine saturation were plotted against I, the trend would be linear on a log-log plot. Currently, no method exists to measure the "electrically effective" brine volume, although imaging techniques would be useful in quantifying the macroscopic distribution of the brine.

Aged-State

Since the study was designed for eventual field application, a practical restoration process was sought which imitates the natural sequence of events in an oil reservoir. It is assumed that the reservoirs in question were originally water-filled and underwent a normal drainage process. Through field production, brine is currently displacing oil.

At the beginning of the experiment, the plugs were at S_{wi}, with brine and crude-oil phases present. Normally, the resistivity of the 100% brine saturated rock (R_O) is measured prior to oil or air displacing water, as in the case of porous-plate drainage experiments. This was not possible, since during the course of the experiment the rock was never 100% brine saturated. The derivation of R_O in the continuous injection experiments is given in the "Laboratory Methods" section of the paper.

Continuous-injection, effective reservoir stress: The distinctive "Knee" and "S" trends may be explained in the following way. The low S_{wi}'s observed in the samples, 4 to 19%, indicate that continuous brine films may not be present. In other words, the saturations are below Melrose's (1982) "critical" brine saturation. Oil-wet behaviour can also be inferred based on Craig's "Rules of Thumb" (1971). As noted in the "Results" section of the paper, the Amott wettability-to-oil increased with ageing. Therefore, the brine possibly exists both as globules in the pores and as discrete patches wetting grains and confined to micropores. This is the fractional wettability condition described by Anderson (1986).

The brine distribution at the start of injection is not homogeneous, if it were, the resistivity would be decreasing as expected in an Archie system. Instead, a flat resistivity trend is observed, implying a poor electrical path through the pore space.

With continuing injection, the brine saturation increases and eventually the discrete brine globules coalesce, improving the electrical path. The immediate improvement in the electrical path is seen as a slope change in the I-S_W plot as seen previously in Figure 15. Since the aged samples are moderately to strongly oil-wet, it is likely that the brine forms continuous channels or fingers, dispacing oil in front of it (Anderson, 1986; Mohanty et al., 1991). As brine saturation continues to increase, I decreases in a "normal" Archie fashion, with the trend becoming linear. In the "S" trend samples, the decrease in resistivity is dramatic and is manifested as a sudden order-of-magnitude resistivity change over 5 to 10 saturation units as previously seen in Figure 16.

Another possible explanation of the non-linear I-S_w relationship has been given by Sprunt et al. (1991). They postulate that changes in I-S_w behaviour are due to a flood front passing between pairs of measuring electrodes, in their "drainage" type measurement. Their tests were made using 4-electrode cells, whereas we used 2-electrode cells.

As with the porous-plate drainage measurements, the curve shape is the result of non-Archie behaviour below a particular S_w. At high brine saturations, S_w is very close to the "electrically-effective" water saturation (S_{wee}), if not the same. However, in the low-water-saturation, non-Archie region, $S_{wee} < S_w$. A non-linear I-S_w trend results from plotting I with an S_w that does not correspond to S_{wee} (Figure 27).

The "Linear" trend is exhibited in samples that conform to Archie's model. It was noted in the "Results" section that this curve type accompanied rocks with lower PGF's and higher S_{wi}'s. Therefore, it follows that a continuous brine film may exist in rocks of this type, thus providing a conductive path from the beginning of the test. In other words, a capillary pressure high enough to cause the stable brine film to break, was not achieved in the initial desaturation prior to ageing. Nor was there significant displacement of brine by crude oil during the ageing process.

Lastly, it has been observed that the modal value in the PGF distribution increases with the "Linear", "S" and "Knee" trends, respectively. The trends may represent a progressive deterioration of electrical continuity, which may be linked to pore geometry. However, the scatter in the PGF data precludes the definitive prediction of curve type from the PGF alone.

PETROPHYSICAL APPLICATIONS

The petrophysicist is charged with evaluating reservoirs, despite non-ideal pore systems. So, pragmatic solutions are often required. The Archie model may not be appropriate for formation evaluation, depending on the brine saturation and distribution. Examination of the I-S_w trend will readily indicate this.

If the Archie model is to be employed, despite potential non-Archie behaviour at low brine saturations, a different approach must be used. The full I-S_W curve is not required in this method to estimate the initial water saturation in the reservoir. This can be done using I at S_{Wi} to derive a 2-point n (Figure 28). It should be noted that the 2-point derived n is usable for calculations only in the saturation region from which it is derived.

Several assumptions are required in this technique.

- The reservoir and laboratory *fluid distributions* must be similar.
- The laboratory fluids must be *representative* of those in the reservoir.
- The laboratory *irreducible water saturation* must be representative of the reservoir.

This approach can be used in reservoirs drilled with oil base mud and should work equally well for those drilled with water-base mud, as long as the mud filtrate invasion does not significantly affect the deep-reading resistivity device. This method is not valid once the reservoir has undergone water flooding since the fluid distributions, and therefore n, will be different.

CONCLUSIONS

- Anomalies occur in resistivity index data when non-Archie conditions prevail.
- Petrophysical evaluation can be accomplished with the Archie model where non-Archie characteristics are evident, if a 2-point saturation exponent (n) is used.
- The entire I-Sw curve is not required for petrophysical evaluation, as long as the reservoir saturations are expected to be in a narrow range. While the electrical behaviour at the other saturations may be interesting and complex, it may be irrelevant.
- "Normal" values of the saturation exponent, 1.8-2.2, are observed in the majority of the samples when using a 2-point method, even in moderately oil-wet rocks.
- The 2-point saturation exponent does not change significantly with increasing stress.

- The saturation exponent increases with effective reservoir stress, if a least-squares fit through the data is used.
- The resistivity of a rock at irreducible brine saturation varies with the wetting condition of the rock.
- The resistivity index becomes non-linear as the conductive brine film becomes discontinuous in tests involving brine de-saturation.
- In continuous injection tests, where brine displaces oil, the resistivity index exhibits a change in slope when the discontinuous brine phase becomes continuous, thereby improving the electrical path.
- A knowledge of electrically effective water saturation (S_{wee}) distribution would be an important addition to further work. Current imaging techniques, however, are unlikely to be of assistance.

NOMENCLATURE

A_{wo} = Amott wettability to oil, dimensionless
A_{ww} = Amott wettability to water, dimensionless
F = formation resistivity factor, dimensionless
I = resistivity index, dimensionless
I_w = USBM wettability index, dimensionless
k = permeability, mD
m = Archie cementation exponent, dimensionless
n = Archie saturation exponent, dimensionless
$\emptyset$ = total porosity, fractional
P_c = capillary pressure
PGF = Pore Geometry Factor, dimensionless
R_o = resistivity of 100% brine saturated rock, ohm-m
R_t = resistivity of partially saturated rock, ohm-m
R_w = connate water resistivity, ohm-m
S_{ro} = residual oil saturation, fractional
S_w = connate water saturation, fractional
S_{wee} = electrically effective water saturation, fractional
S_{wi} = irreducible water saturation, fractional

ACKNOWLEDGEMENTS

We would like to thank Mobil North Sea Ltd for permission to publish this paper. We also thank David Herrick, David Kennedy and Eve Sprunt of Mobil Research and Development Corporation for their critical review and suggestions during the writing of the paper.

REFERENCES

Anderson, W., G., 1986, Wettability Literature Survey- Part 1: Rock/Brine/Oil Interactions and the Effects of Core Handling on Wettability, *Journal of Petroleum Technology,* October, p. 1125-1144.

Anderson, W., G., 1986, Wettability Literature Survey- Part 3: The Effects of Wettability on the Electrical Properties of Porous Media, *Journal of Petroleum Technology,* December, p. 1371-1378.

Craig, F., F., 1971, *The Reservoir Engineering aspects of Water Flooding*, Monograph Series, SPE, Richardson, Texas, No. 3.

de Waal, J., A., Smits, R., M.,, M., Schipper, B., A.,, 1991, Measurement and Evaluation of Resistivity-index Curves: *The Log Analyst,* v. 32, no. 5, September-October, p. 583-595.

Donaldson, E., C., Siddliqui, T., K., 1989, Relationship Between the Archie Saturation Exponent and Wettability: *SPE Formation Evaluation,* v. 4, no. 3, September, p.359-362.

Herrick, D., C.,,1988, Conductivity Models, Pore Geometry, and Conduction Mechanisms, Paper D *in* Twenty -Ninth Annual Logging Symposium, San Antonio,Texas, Transactions, Society of Professional Well Log Analysts.

Keller, G., V., 1953, Effect of Wettability on the Electrical Resistivity of Sand: *The Oil and Gas Journal*, January, p. 62-65.

Lenormand, R., Zarcone, C., 1988, Physics of Blob Displacement in a Two-Dimensional Porous Medium: *SPE Formation Evaluation*, March, p. 271-275.

Leverett, M., C., 1941, Capillary Behavior in Porous Solids, Trans., AIME, v. 142, p159.

Longeron, D., G., 1989, Effect of Overburden Pressure and the Nature of Microscopic Distribution of Fluids on Electrical Properties of Rock Samples: *SPE Formation Evaluation*, v. 4, no. 2, June, p. 194-202.

Longeron D. G., Bouvier L.,1989, Resistivity index and Capillary Pressure Measurements Under Reservoir Conditions Using Crude Oil, SPE 19589, *in* Annual Conference and Exhibition, Formation Evaluation and Reservoir Geology, Proceedings, p. 187-200.

Lyle, W., D., Mills, W., R., 1989, Effect of Nonuniform Core Saturation on Laboratory Determination of the Archie Saturation Exponent: *SPE Formation Evaluation,* v. 4, no. 1, March, p. 49-52.

Mahmood, S., M., Maerefat, N., L., Chang, M-M., 1991, Laboratory Measurements of Electrical Resistivity at Reservoir Conditions: *SPE Formation Evaluation,* v. 6, no. 3, September, p. 291-300.

Melrose, J., C., 1982, The Interpretation of Mixed Wettability States in Reservoir Rocks, SPE 10971, *in* Annual Fall Technical Conference and Exhibition, Proceedings, Society of Petroleum Engineers of AIME.

Mohanty, K., K., Miller, A., E., 1991, Factors Influencing Unsteady Relative Permeability of a Mixed-Wet Reservoir Rock: *SPE Formation Evaluation*, v. 6, no. 3, September, p. 349-358.

Mungan, N., Moore., E., J., 1968, Certain Wettability effects on Electrical Resistivity in Porous Media: *The Journal of Canadian Petroleum Technology,* January-March, p. 20-25.

Nieto, J., A., Yale, D., P., Evans, R., J., 1990, Improved Methods for Correcting Core Porosity to Reservoir Conditions, Paper F *in* Transactions of the Thirteenth European Formation Evaluation Symposium, Budapest, Hungary, Transactions, Society of Professional Well Log Analysts.

Sharma, M., Garrounch, A., Dunlap, H. F., 1991, Effects of Wettability, Pore Geometry, and Stress on Electrical Conduction in Fluid-Saturated Rocks: *The Log Analyst*, v. 32, no. 5, September-October, p. 511-526.

Soendenaa, A., Bratteli, F. , Kolltveit, K., Normann, H. P., 1989, A Comparison Between Capillary Pressure Data and Saturation Exponent Obtained at Ambient Conditions and at Reservoir Conditions, SPE 19592, *in*Society of Petroleum Engineers Annual Technical Conference and Exhibition, Formation Evaluation and Reservoir Geology, Proceedings, p. 213-225.

Sprunt, E., S., Desai, K., P., Coles, M., E., Davis, R., M., Muegge, E., L., 1991, CT-Scan-Monitored Electrical-Resistivity Measurements Show Problems Achieving Homogeneous Saturation: *SPE Formation Evaluation,* v. 6, no. 2, June, p. 134-140.

Sprunt, E., S., 1991, Quality Control of special Core Analysis Measurements, Paper 3RC-96, Preprints Third annual International reservoir Characterisation Technical Conference, DOE Conf 911125, Nov. 3-5, 1991, Tulsa, OK, .

Swanson, B., F., 1985, Microporosity in Reservoir Rocks: Its Measurement and Influence on Electrical Resistivity: *The Log Analyst*, v. 26, no. 6, November-December, p. 42-52.

Wei, Jun-Zhi, Lile, O., B., Influence of Wettability on Two- and Four-Electrode Resistivity Measurements on Beria Sandstone Plugs: *SPE Formation Evaluation*, v. 6, no. 4, p. 470-476.

Worthington, P., F., Toussaint-Jackson, J., E., Pallatt, N., 1988, Effect of Sample Preparation upon Saturation Exponent in the Magnus Field, U.K. North Sea: *The Log Analyst*, v. 29, no. 1, January-February, p. 48-53.

Worthington, P., F., Toussaint-Jackson, J., E., Pallatt, N., 1989, Influence of Microporosity on the Evaluation of Hydrocarbon Saturation.: *SPE Formation Evaluation*, v. 4, no. 2, June, p. 203-209.

Worthington, P., F., Evans, R., J., Klein, J., D., Walls, J., D., White, G., 1990, SCA Guidelines for Sample Preparation and Porosity Measurement of Electrical Resistivity Samples, Part 3- The Mechanics of Electrical Resistivity Measurements on Rock Samples: *The Log Analyst*, v. 31, no. 2, March-April, p. 64-67.

APPENDIX

SAMPLE PREPARATION

Sample selection: The sample selection for this project was made after reviewing core from seven wells. The initial aim was to select representative cores from eight formations. In order to realise these aims, it was necessary to cut a limited number of samples from unpreserved cores although the majority of samples drilled from cores that had been stored by immersion in either oil or brine.

Routine core analysis data and downhole logs were used to select suitable horizons. The plug locations and orientations were selected by a sedimentologist. When this work began it was uncommon to use CAT scanners in commercial core analysis and consequently CAT scanning was not used.

Plug samples were drilled from the selected cores and trimmed into right cylinders using brine as the coolant/lubricant for the diamond tipped cutting tools. All of the samples were $1\frac{1}{2}$-inches in diameter, but the sample length varied from $1\frac{1}{2}$ to $2\frac{1}{2}$-inches.

Sample cleaning: Hydrocarbons and brine were removed from the plug samples using soxhlet extraction. The solvents were trichloroethane, and azeotrope of chloroform:methanol and methylamine followed by methanol alone. The plugs were considered to be clean when refluxing solvents examined with ultraviolet light showed no hydrocarbons and no silver chloride precipitate formed when the methanol was reacted with silver nitrate.

Wettability data on the cleaned core indicated that the cleaning did not always render the plugs strongly water wet.

After the samples were considered to be clean they were dried in a vacuum oven at $60^{o}C$ until constant weights were attained. The samples were then stored in a dessicator.

Determination of porosity and permeability: Porosity and permeability of each sample were determined prior to saturating the plugs with brine.

The grain volume of the plugs was determined using the expansion of helium. Gas permeability was determined by flowing nitrogen through the plugs whilst they were mounted in Hassler cells with a 250 psi confining pressure.

Final sample selection: The final sample test suite was chosen after reviewing the permeability and porosity data and the physical condition of the plugs. Heterogeneous samples were eliminated from the test group.

Brine preparation: Two synthetic formation brines were prepared, each approximating the composition of the field waters. The Jurassic brine had a resistivity of 0.096 ohm-m at 20°C and the Triassic 0.088 ohm-m. The brines were prepared in 40L batches, filtered (10 micron pre-filter and 0.45 micron filter) and decanted into storage vessels. As each batch of brine was prepared, sub-samples were taken and degassed so that density, viscosity and resistivity could be determined. The density was determined at five temperatures using a Paar densiometer. The viscosity was determined using a falling ball viscometer and resistivity was measured using a flow-through Metrohm type cell.

Sample saturation: The selected plugs were saturated using a three stage procedure. The plugs were placed into an airtight vessel and the system was evacuated to 0.005 mbar. In an adjoining vessel filtered brine was also evacuated. The brine was then introduced into the vessel containing the plugs and the pressure in the system was increased up to 1600 psi. and maintained for 24 hours prior to releasing the pressure.

At this juncture the bulk volumes of the samples were measured and the pore volumes were calculated. This value was then compared with the pore volume determined by the weight increase due to the plug saturation process. The samples were then stored immersed in a container that had been filled with filtered, degassed saturant.

FORMATION RESISTIVITY FACTOR AT ROOM CONDITIONS

Once the samples had been saturated, the room condition formation resistivity factors (F) were measured.

Individual plugs were removed from their storage vessel and excess surface brine was removed from the plugs by wiping with a non-absorbent cloth. Each sample was then weighed and placed into an assembly that permitted the determination of core resistance using the 4- terminal system. During this process the current density was set at 0.1 mAmps/cm^2 and the current frequency was altered until the phase angle obtained was at a minimum.

After reviewing the initial data, a frequency of 1000 Hz was selected and used for all core resistivity measurements. The phase angle varied from 0 to 0.3 degrees. A Genrad Digibridge was used for this operation.

The R_O of the samples were determined after leaving them immersed in brine from seven days. They were then stored (immersed in brine) for a further seven days before the second measurement. Subsequent measurements over a three day period varied by less than 2 percent.

AIR-BRINE CAPILLARY PRESSURE AND FORMATION RESISTIVITY INDEX AT ROOM CONDITIONS

When the samples and the F values had stabilised, the capillary pressure curves were determined using the porous-plate system with gas as the non-wetting phase. Once the sample had attained equilibrium saturation at each pressure, the core resistance was measured and Resistivity index (I) calculated.

To determine the capillary pressure curves a group of samples of similar permeabilities were mounted onto ceramic plates using tissue and diatomaceous earth to create capillary contact between the plate and the sample. The porous-plates had been saturated with formation brine by flushing through the plate. The break-through pressure of the plate was selected to be greater than the gas pressure that would be applied during the initial stages of the tests. Prior to loading the plugs into the cell they were weighed.

After sealing the plugs into the capillary pressure cell, a gas cap was applied to the plugs. Brine production was observed as the samples desaturated. After leaving the system for 4 to 5 days the samples were removed from the cell and weighed. The sample desaturation was calculated from the loss of weight. The plugs were then returned to the cell and the pressure reapplied. This process was repeated until the saturation appeared to be stable. At this juncture the core resistance was measured.

The samples were then returned to the cell and additional desaturation was promoted by increasing the pressure of the gas cap. This operation was undertaken using a series of pressures up to 200 psi. During the process, the ceramic plates were changed so that the break-through pressure corresponded to the displacement pressure that was being applied.

Upon completion of the test, the samples were immersed in brine and the system was evacuated. Weight checks were used to gauge the efficiency of the resaturation process.

MEASUREMENTS AT EFFECTIVE RESERVOIR STRESS

The samples were to be tested to determine *F* and *Pc/I* at effective reservoir stress. In order to facilitate these measurements, the plugs were mounted in an assembly that includes a ceramic disc, silver current electrodes and silver voltage electrodes that encircle the core at two points. The resistance was measured using a 4-terminal system.

Firstly, the plugs were wrapped with two layers of PTFE tape along 1 cm section of their length from each end. Using the ridge created by the PTFE, silver electrodes were butted to the surface of the core and then held into position using PTFE tape. This assembly was then loaded into a Viton rubber sleeve. At one end of the plug a tissue filter, ceramic disc and silver membrane filter were positioned prior to being held in position by the floating platen. The other end of the plug was fitted onto the fixed platen again using a silver filter at the current electrode.

The potential electrodes were connected to lead-through connectors that are mounted in the fixed platen.

During this operation an unquantified volume of brine was introduced into the system, between the rubber sleeve and core. Before any true resistance measurements could be determined this brine had to be removed from the system. This was achieved by increasing the confining pressure in 10 psi increments and monitoring the fluid produced by the core resistance. This information was used to determine sleeve conformance and the point at which pore volume compaction started.

The confining pressure was then increased and pore volume change and *F* were determined at salient points up to a maximum of 5100 psi and the core was held at these conditions for 10 days.

At this juncture, a gas cap was applied to each sample and the capillary pressure curve was determined using a series of pressures. Equilibrium saturations were determined by monitoring the brine produced from each sample, and *I* was determined at each salient point.

Upon completion of this phase the confining pressure was released and the samples were removed from the cell. The final water saturation was determined using Dean and Stark extraction.

SAMPLE AGEING

The samples were then saturated with brine using the same procedures used during sample preparation. The initial water saturation was established by a single pressure (200 psi) stage desaturation using the porous-plate method. Re-saturation of the plugs was achieved by cooling them to 6° C in an adapted refrigerator and by drawing in crude oil under vacuum. The efficiency of the procedure was checked by making mass balance calculations. They were then transferred into a sealed chamber to allow the cores to age. The samples were held at reservoir temperature, 200°F, for approximately 1000 hours.

FORMATION RESISTIVITY INDEX BY CONTINUOUS INJECTION

After ageing the samples were loaded into individual core holders and an effective reservoir stress was applied until the cores were sustaining 5100 psi. During this operation the plugs were loaded into a Viton rubber sleeve and silver membrane filters placed at each end of the plug. The 0.45 micron silver filters that were used as electrodes were 0.05 mm in thickness. In this application the filter does not exert any influence on the dynamic properties of the test. Core resistance was determined before and after flushing brine across the face of the sample. Brine was then injected into the core at a rate equivalent to one pore volume throughput over a 14 day period. As the brine saturation increased, the core resistance was recorded. These data were used to calculate I at effective reservoir stress.

ADDITIONAL RESISTIVITY MEASUREMENTS

Upon completion of the continuous injection measurements, the samples were re-cleaned, saturated, desaturated and S_{wi} redetermined. The cores were then loaded into individual core holders and core resistance determined, with the plugs at 5100 psi.

TABLE 1

ROCK PARAMETERS

FULL DATA SET

	Jurassic	Triassic
Samples	42	21
Avg Porosity %	16.5	17.2
Range	12.9-23.1	14.2-24.6
Median	15.8	19.7
Std Dev	2.69	13.02
Avg K_{air} mD	556	228
Range	29-4580	6.9-887
Median	151	62.5
Std Dev	1113	298
Avg Q_v meq/CC	0.131	0.104
Range	0.035-0.228	0.032-0.205
Median	0.124	0.091
Std Dev	0.064	0.055
Avg Grain Den	2.65	2.66
Range	2.63-2.68	2.64-2.68
Median	2.65	2.66
Std Dev	0.012	0.013

TABLE 2

ROCK PARAMETERS
CLEANED-STATE POROUS-PLATE DATA

AMBIENT CONDITIONS

	ANOMALOUS	LINEAR	DISCONTINUOUS
Samples	9	10	11
Avg Porosity %	19	17	16
Range	15-25	13-22	13-19
Median	19	17	15
Std Dev	3	3	2
Avg PGF	4.6	4.0	2.8
Range	0.79-14	0.67-11	1.3-4.1
Median	3.9	3.1	2.6
Std Dev	4.3	3.3	0.92
Avg K_{air}, mD	826	506	134
Range	12-4580	7-2720	29-260
Median	264	136	118
Std Dev	1466	846	76
Avg S_{wi}	18	17	17
Avg A_{ww}	0.13	0.16	0.19
Avg A_{wo}	0.05	0.17	0.12
Avg Q_v, meq/CC	0.089	0.123	0.142

TABLE 3

ROCK PARAMETERS
CLEANED-STATE POROUS PLATE DATA

EFFECTIVE RESERVOIR STRESS

	ANOMALOUS	LINEAR
Samples	11	14
Avg Porosity %	19	16
Range	13-25	13-20
Median	19	16
Std Dev	4	2
Avg PGF	5.5	2.6
Range	0.79-14	0.67-4.1
Median	4.5	2.6
Std Dev	4.3	1.1
Avg K_{air}, mD	1027	130
Range	12-4580	7-304
Median	457	112
Std Dev	1428	90
Avg S_{wi}	15	18
Avg A_{ww}	0.11	0.21
Avg A_{wo}	0.12	0.11
Avg Q_v, meq/CC	0.100	0.132

TABLE 4

ROCK PARAMETERS
AGED DATA, CONTINUOUS INJECTION

EFFECTIVE RESERVOIR STRESS

	KNEE	S	LINEAR	ANOMALOUS
Samples	16	6	4	4
Avg Porosity %	18	17	17	18
Range	14-24	13-21	15-19	15-22
Median	16	15	18	16
Std Dev	3	3	2	4
Avg PGF	3.3	4.5	0.95	6.8
Range	0.9-7.9	1.8-10.1	0.49-1.7	3.8-15
Median	3.1	2.6	0.82	4.3
Std Dev	1.8	3.6	0.50	5.3
Avg K_{air}, mD	277	611	19	1422
Range	12-1120	47-2200	5-50	234-4880
Median	180	102	12	286
Std Dev	295	892	21	2306
Avg S_{wi}	12	11	28	12
Avg A_{ww}	0.05	0.03	0.07	0.01
Avg A_{wo}	0.50	0.62	0.58	0.52
Avg Q_v, meq/CC	0.111	0.158	0.187	0.066

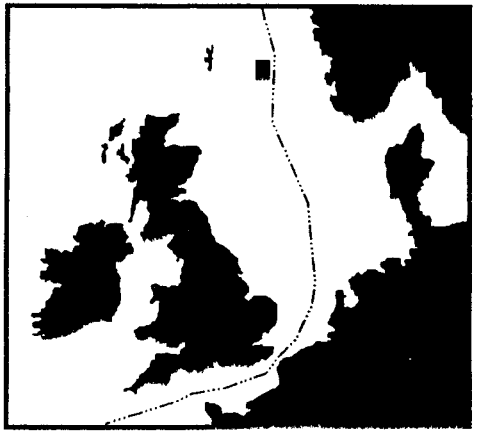

Figure 1 : Location Map

Figure 2. Formation Resistivity Factor at room conditions, two or four wire method.

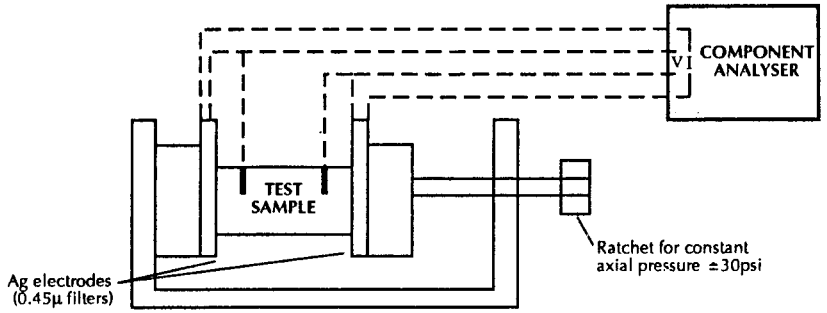

Figure 3. Formation Resistivity Factor at confining stress and Formation Resistivity Index in conjunction with capillary pressure, air-brine, porous plate system.

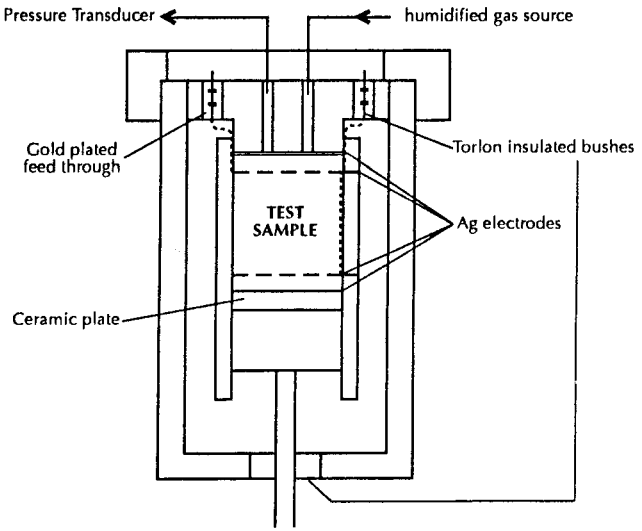

Figure 4. Formation Resistivity Factors at confining pressure and Formation Resistivity Index by fluid injection.

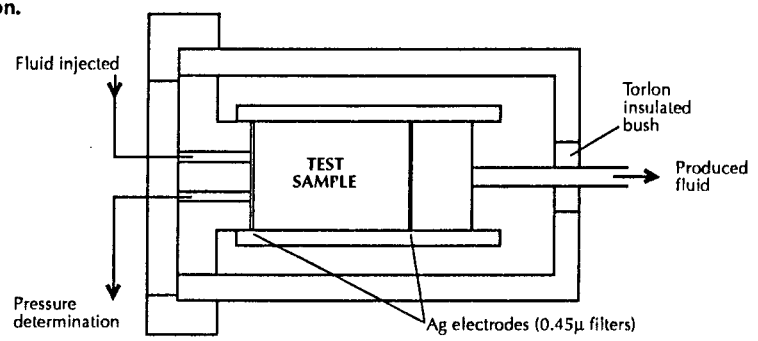

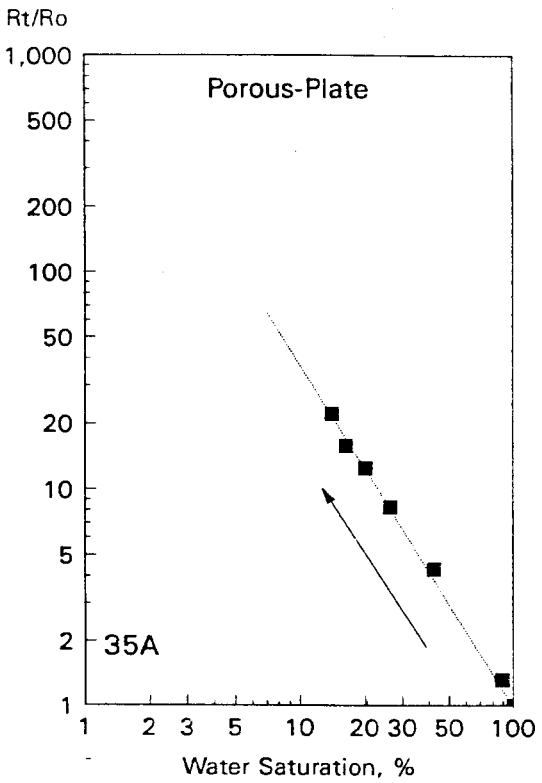

Figure 5: 'Linear' resistivity index. Cleaned, ambient conditions.

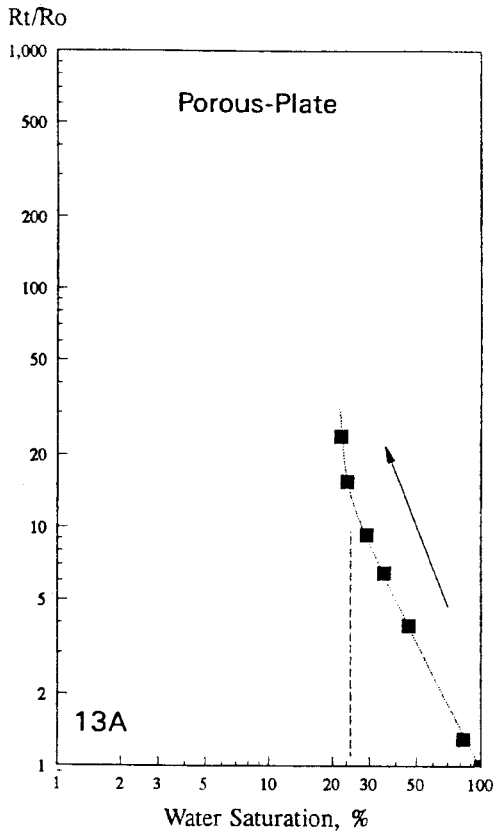

Figure 6:'Discontinuous' resistivity index. Cleaned, ambient conditions.

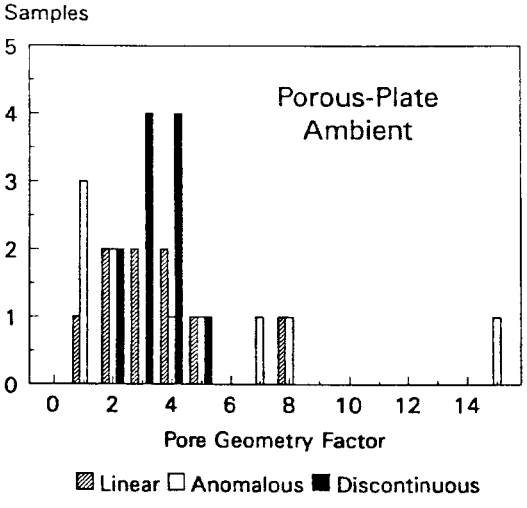

Figure 7: Pore Geometry Factor distributions by trend. Cleaned plugs.

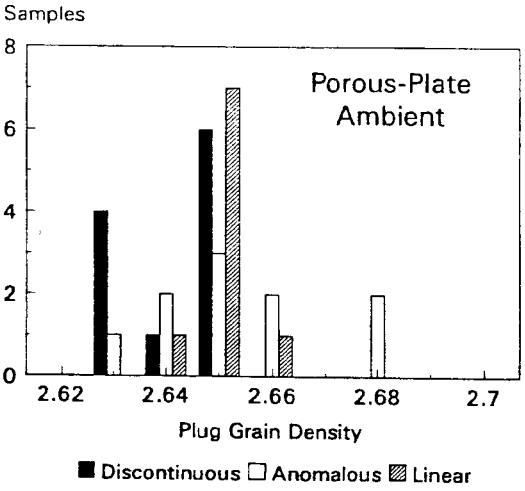

Figure 8: Grain density distributions by "trend". Cleaned plugs.

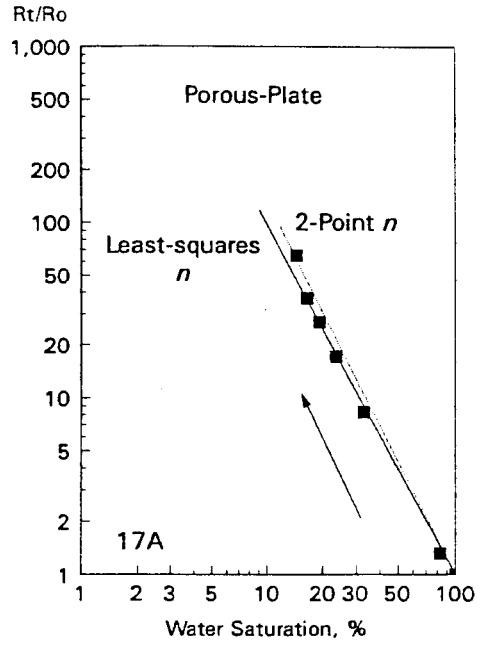

Figure 9: Least squares and 2-point saturation exponents. Increase in *n* using 2-point method. Cleaned plugs, ambient conditions.

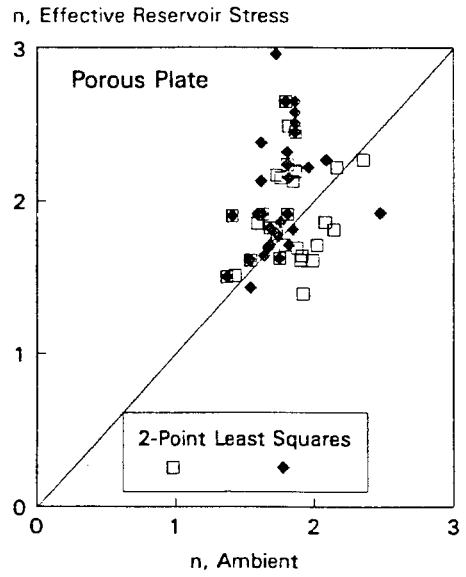

Figure 10: Comparison of two-point and least-squares derived saturation exponents. Entire data set used. Cleaned plugs.

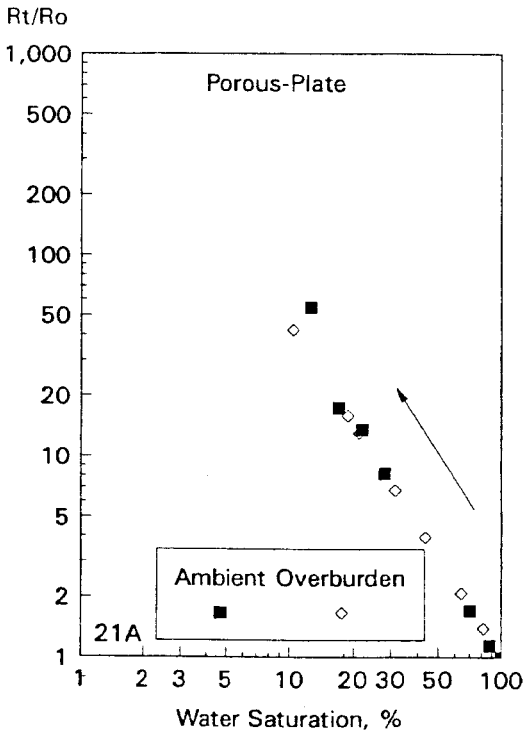

Figure 11: Change in 'Discontinuous' trend with effective reservoir stress. Cleaned plugs.

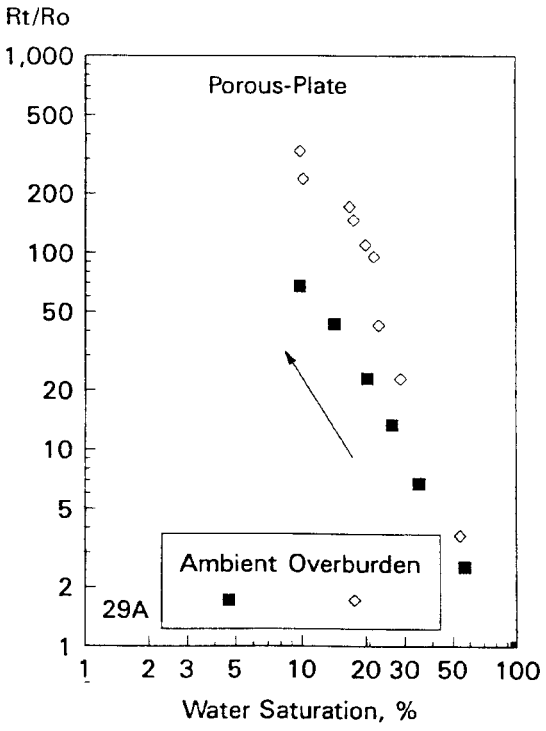

Figure 12: Change in 'Anomalous' data with effective reservoir stress. Cleaned plugs.

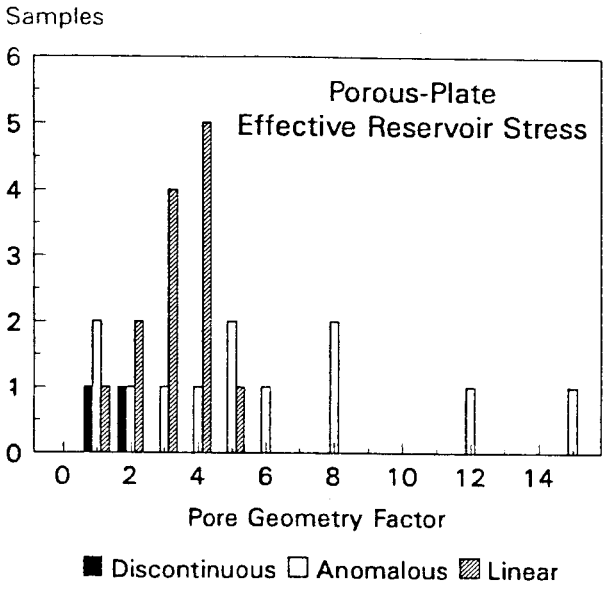

Figure 13: Pore Geometry Factor distributions for samples exhibiting trends. Cleaned plugs,

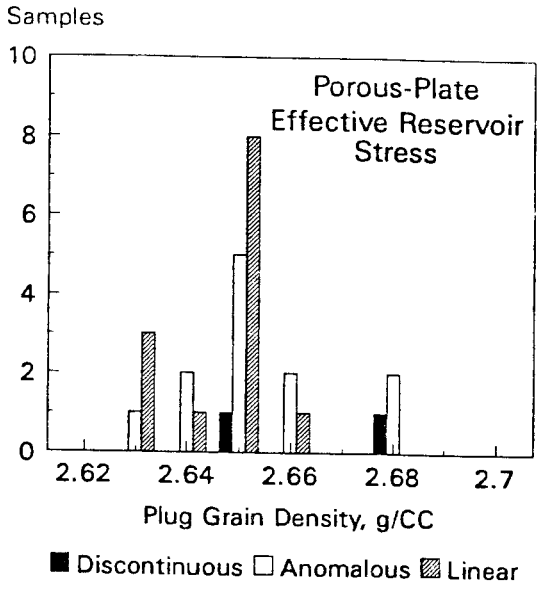

Figure 14: Distributions of plug grain densities for *I-Sw* trends. Cleaned plugs.

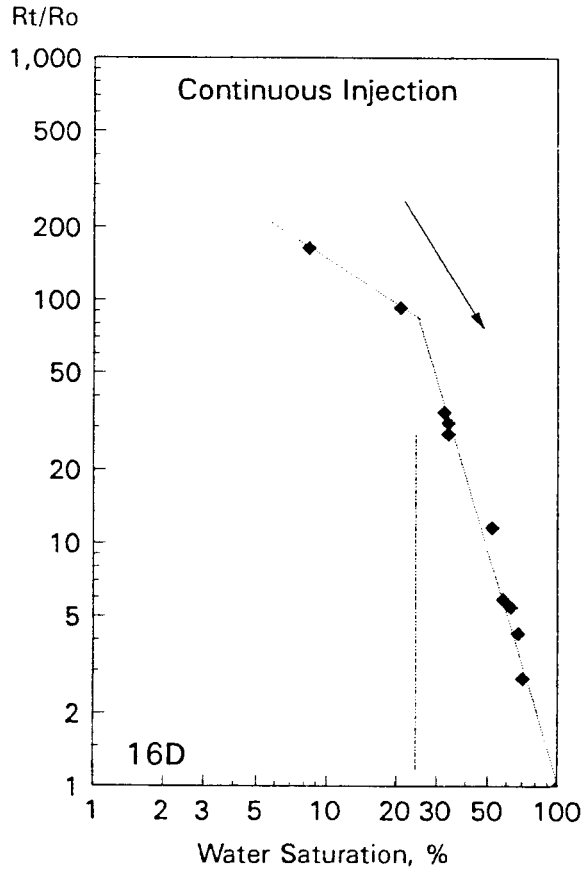

Figure 15: "Knee" resistivity index. Aged-state at effective reservoir stress.

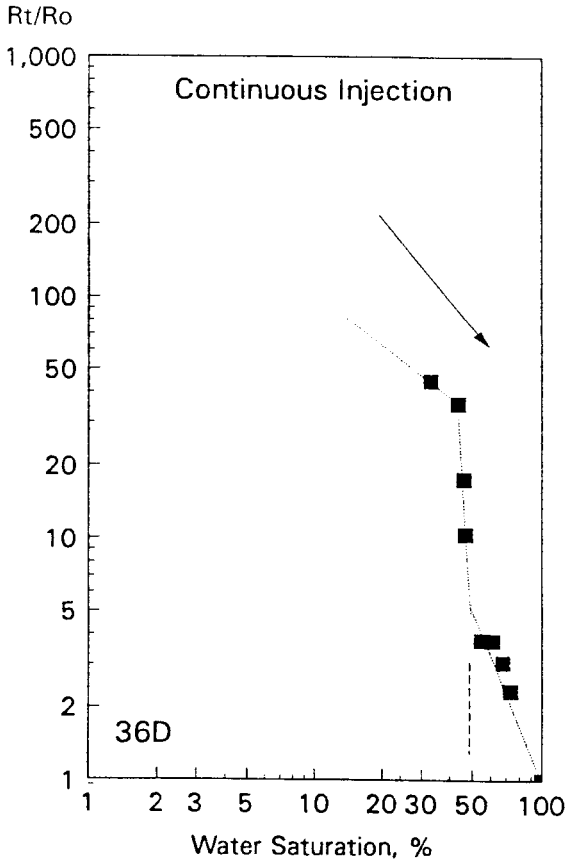

Figure 16: "S" resistivity index. Aged-state at effective reservoir stress.

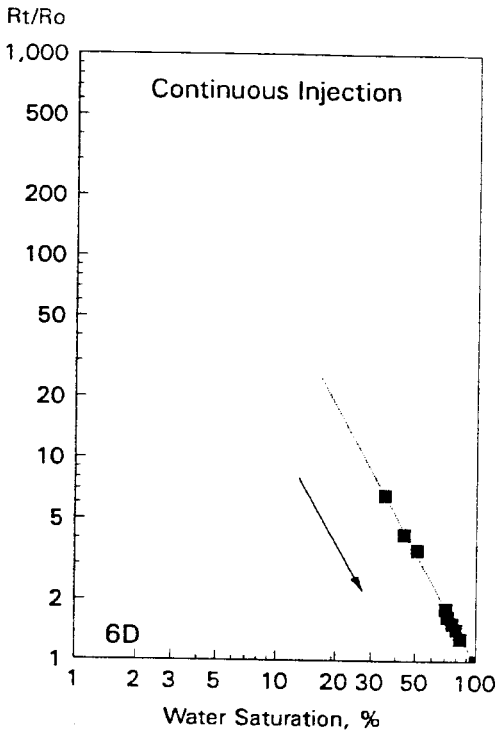

Figure 17: 'Linear' resistivity index. Aged-state at effective reservoir stress.

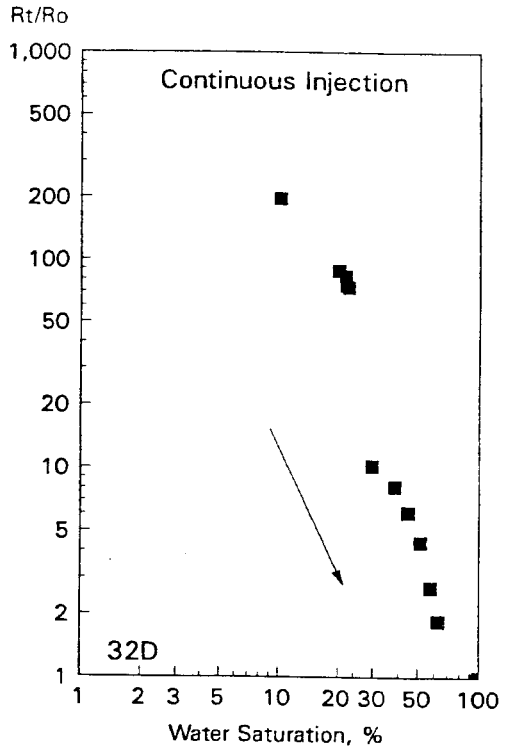

Figure 18: 'Anomalous' resistivity index. Aged-state at effective reservoir stress.

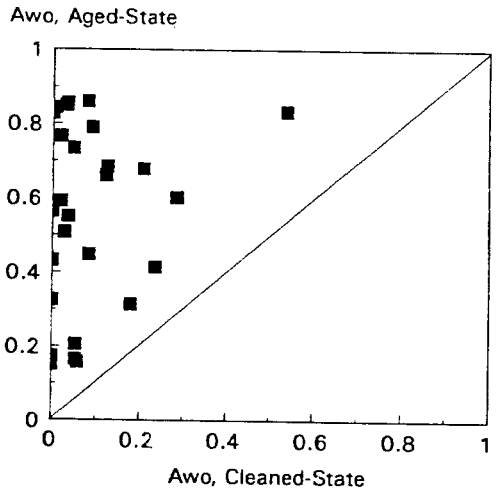

Figure 19: Amott wettability-to-oil, cleaned versus aged samples from same depths.

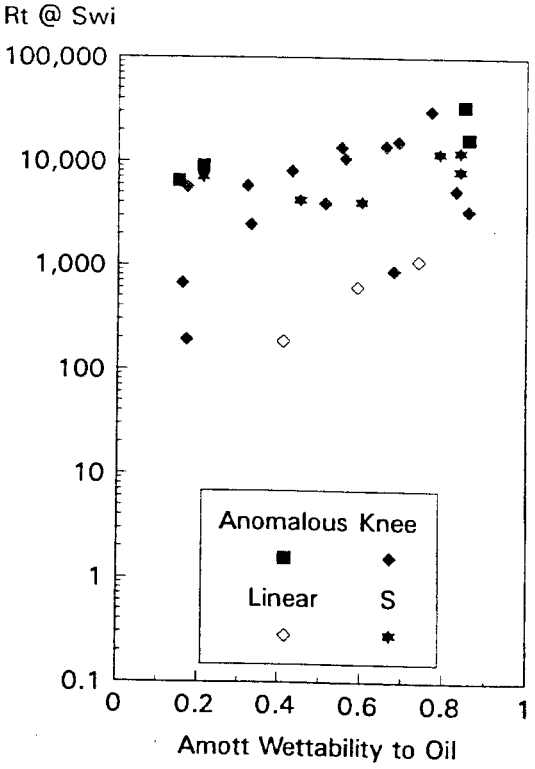

Figure 20: Relationship of plug resistivity with Amott wettability-to-oil. Aged plugs.

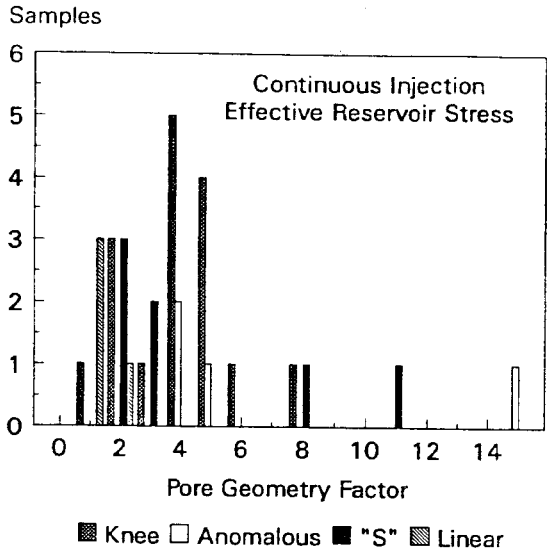

Figure 21: Distributions of Pore Geometry Factors for I-Sw trends. Aged plug sets.

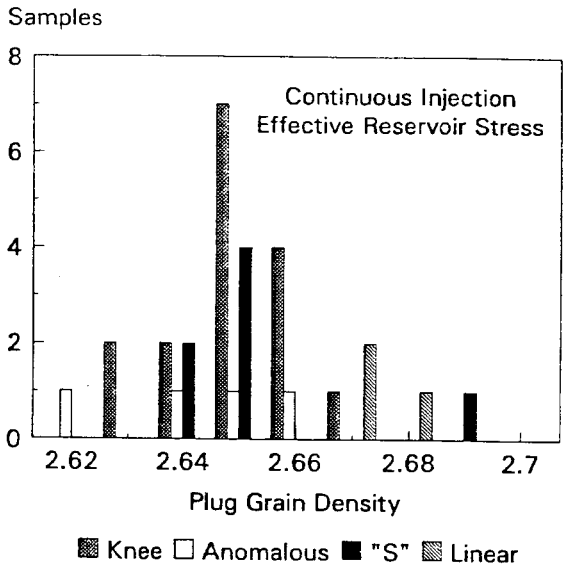

Figure 22: Distributions of plug grain densities for I-Sw trends. Aged plugs.

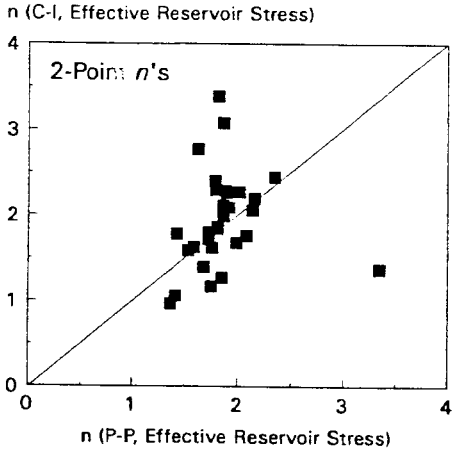

Figure 23: Comparison of 2-point *n*'s from porous-plate and continuous injection tests. Twinned samples used. Porous-plate plugs are clean, continuous injection plugs are aged.

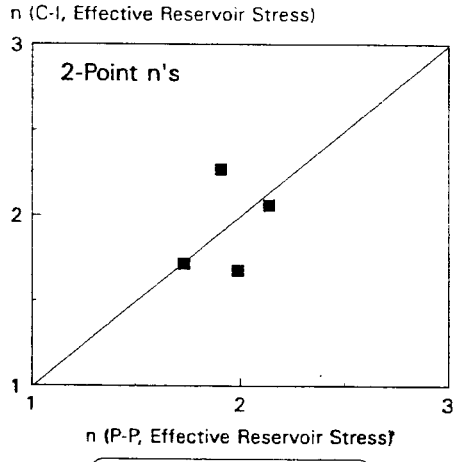

Sample	PGF
8A/8D	1.33/ 1.33
16A/16D	3.11/3.08
18A/18D	1.67/1.66
21A/21D	4.12/4.12

Figure 24: Comparison of 2-Point n's from porous-plate and continuous injection tests. Data from twinned samples with less than 1% difference in Pore Geometry Factors.

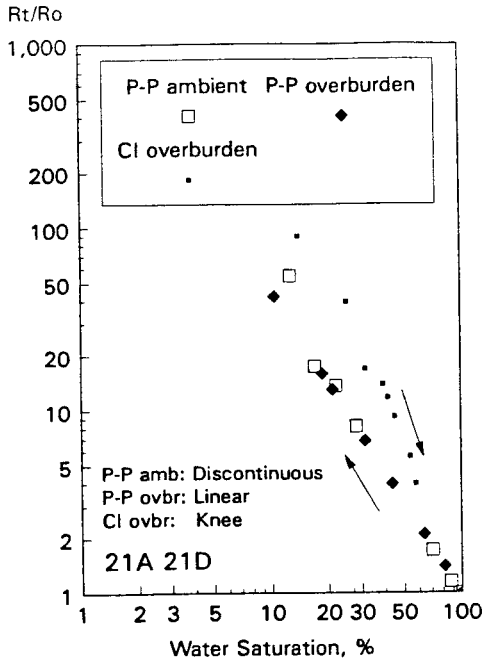

Figure 25: Comparison of "trends" from samples at same depth. *Sw* is decreasing in the porous-plate test, and increasing in the continuous injection test. Overburden = Effective Reservoir Stress.

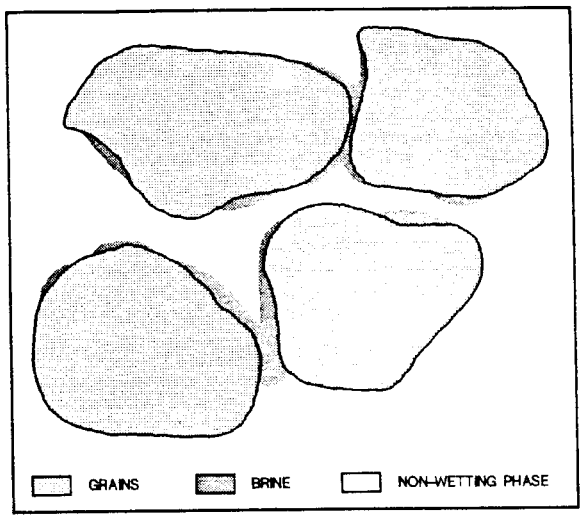

Figure 26 : Conceptual view of pore space at very low brine saturation. Non-wetting phase in contact with grains. Discontinuous electrical path.

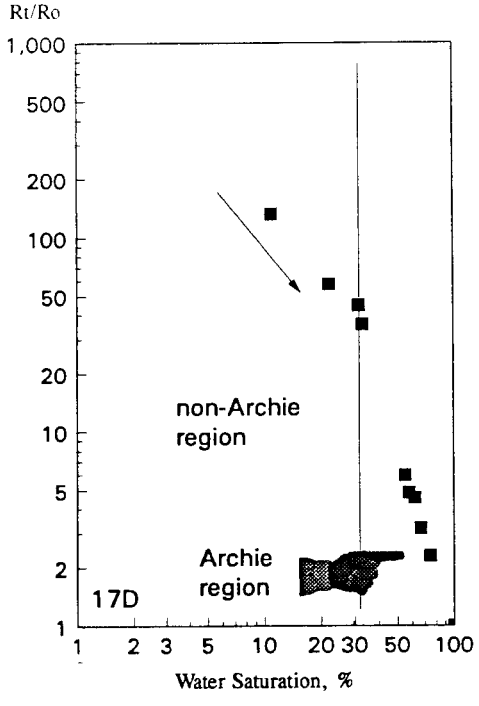

Figure 27: Resistivity index plot showing Archie and non-Archie regions. Aged-state, continuous injection at effective reservoir stress.

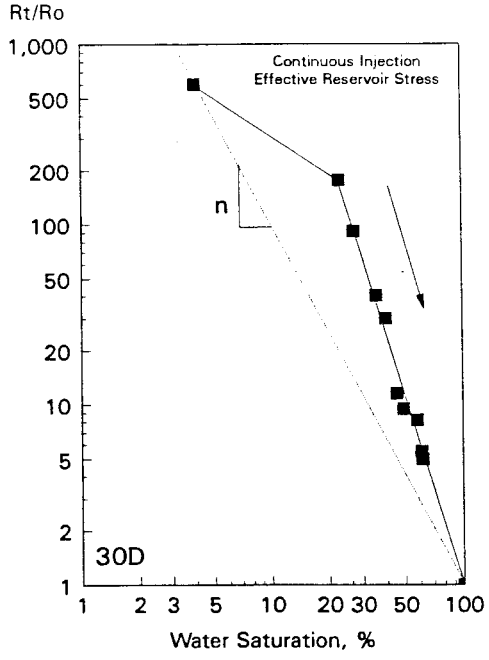

Figure 28: Saturation exponent at *Swi* using the 2-point method.